

*Letter to the Editor***A VLT colour image of the optical Einstein ring 0047–2808\*****S.J. Warren<sup>1</sup>, G.F. Lewis<sup>2</sup>, P.C. Hewett<sup>3</sup>, P. Møller<sup>4</sup>, P. Shaver<sup>4</sup>, and A. Iovino<sup>5</sup>**<sup>1</sup> Blackett Laboratory, Imperial College of Science Technology and Medicine, Prince Consort Rd, London SW7 2BZ, UK (s.j.warren@ic.ac.uk)<sup>2</sup> Department of Physics and Astronomy, University of Victoria, PO Box 3055, Victoria BC, V8W 3P7, Canada (gfl@almuhit.phys.uvic.ca) and Astronomy Department, University of Washington, Box 351580, Seattle, WA 98195-1580, USA<sup>3</sup> Institute of Astronomy, Madingley Road, Cambridge CB3 0HA, UK (phewett@ast.cam.ac.uk)<sup>4</sup> European Southern Observatory, Karl-Schwarzschild-Strasse 2, D-85748 Garching bei München, Germany (pmoller; pshaver@eso.org)<sup>5</sup> Osservatorio Astronomico di Brera, Via Brera 28, I-20121 Milano, Italy (ovino@brera.mi.astro.it)

Received 1 December 1998 / Accepted 19 January 1999

**Abstract.** The optical Einstein ring 0047 – 2808 was imaged by the VLT UT1 during the science verification programme. The ring is the image of a high-redshift  $z = 3.595$  star-forming galaxy, with strong Ly $\alpha$  emission at 5589Å, gravitationally lensed by a massive early-type galaxy at  $z = 0.485$ . Relative to earlier NTT data the high signal-to-noise ratio of the VLT Ly $\alpha$  narrow-band image allows much improved constraints to be placed on the surface-brightness profile of the source and on the mass, leading to a measured mass-to-light ratio of  $M/L_B \sim 13 h$  for the deflector galaxy. We have combined the VLT  $B$ -band and Ly $\alpha$  narrow-band images with a  $K$ -band image obtained at UKIRT to produce a deep colour image of the system.

**Key words:** galaxies: formation – cosmology: gravitational lensing

**1. Introduction**

Einstein-ring gravitational lens images should be much more common at optical wavelengths than at radio wavelengths (Miralda-Escudé and Lehár 1992), but so far all but one of the known Einstein rings have been discovered by radio techniques. The exception is 0047–2808 (Warren et al. 1996a) where a high-redshift  $z = 3.595$  star-forming galaxy, with strong Ly $\alpha$  emission at 5589Å, is lensed by a massive early-type galaxy at  $z = 0.485$ . We are engaged in a survey to detect similar systems (Warren et al. 1996b). The search strategy is to identify anomalous emission lines (Ly $\alpha$  from star-forming galaxies at  $2 < z < 4$ ) in the spectra of a large sample of distant early-type galaxies at  $z \sim 0.4$ . This has the advantage that by the very nature of the identification procedure the redshifts of both the source and deflector are obtained and so the full lensing

geometry is known. In addition, because the sources are extended the resulting images, rings or arcs, offer the prospect of providing powerful constraints on the mass distribution in the deflecting galaxies (Kochanek 1995). Finally, because of the magnification, it is possible to study these very faint sources both spectroscopically (Warren et al. 1998) and morphologically, resolving angular scales much smaller than is possible for unlensed objects. The latter prospects are of particular interest because the sources are similar to but fainter than the population of high-redshift star-forming objects identified by Steidel and coworkers (Steidel et al. 1996), and cannot presently be studied in any other way. In this paper we present VLT UT1 broad- and narrow-band imaging, together with UKIRT  $K$ -band imaging of 0047–2808.

**2. Observations and data reduction***2.1. VLT imaging*

Broad-band  $B$  and Ly $\alpha$  narrow-band images of 0047–2808 were obtained on the night of 1998 August 30, with the VLT UT1 test camera as part of the Science Verification programme (Leibundgut et al. 1998). The CCD pixel size is  $0''.045$ . However the CCD was binned  $2 \times 2$ , so the pixel size in all the frames was  $0''.09$ . The narrow-band filter has a central wavelength 5589Å and width 20Å FWHM. Integration times were  $3 \times 300$  sec ( $B$ ) and  $3 \times 1200$  sec (Ly $\alpha$ ). The seeing was  $0.6 - 0.7''$ . Procedures followed for bias subtraction and flatfielding were mostly standard. However the flatfielded narrow-band images required a correction for large-scale gradients. This was achieved by firstly combining the deregistered frames, clipping out objects. The resulting frame was smoothed, and normalised, and the flatfielded frames were divided by this correction frame.

*2.2. UKIRT imaging*

Broad-band  $K$  images of 0047–2808 were obtained with the UKIRT IRCAM3 instrument on the nights of 1997 Septem-

*Send offprint requests to:* S.J. Warren

\* Based on observations obtained at the European Southern Observatory, Paranal, Chile, and the United Kingdom Infrared Telescope, Hawaii

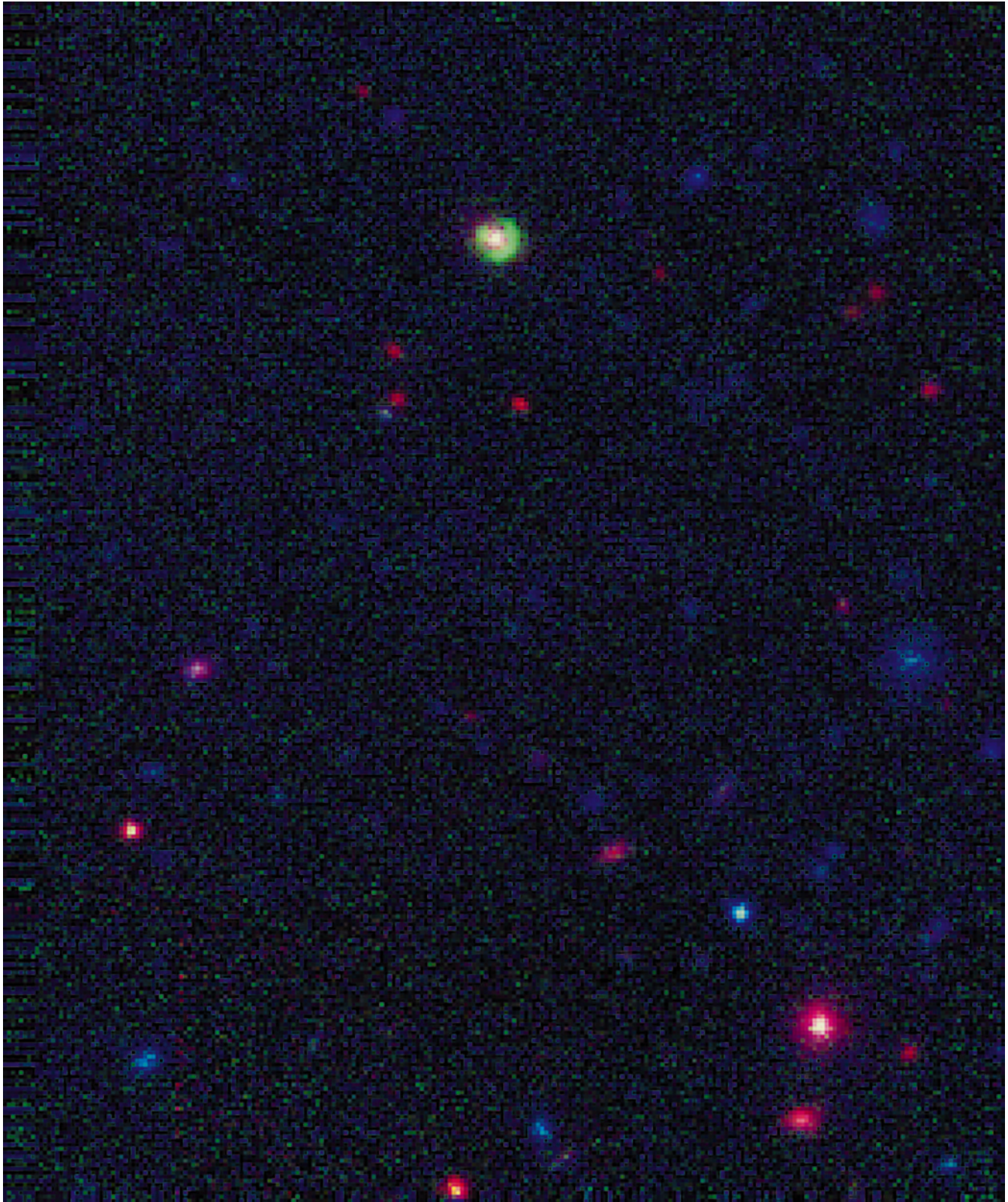


**Fig. 1.** True-colour image of the field of the Einstein–ring gravitational lens 0047–2808, showing a region  $68'' \times 81''$ . North is up and East to the left. The image is a *rgb* combination of the VLT *B* and narrow-band images and the UKIRT *K* image. Because of the strong Ly $\alpha$  emission line in the narrow-band the ring ( $z = 3.595$ ) appears as green. The lensing galaxy ( $z = 0.485$ ) is red because the galaxy is bright in the *K* band but faint in the *B* and narrow bands. There is a second massive elliptical galaxy in the field, visible as the brightest red image in the SW quadrant, which has a redshift  $z = 0.488$ .

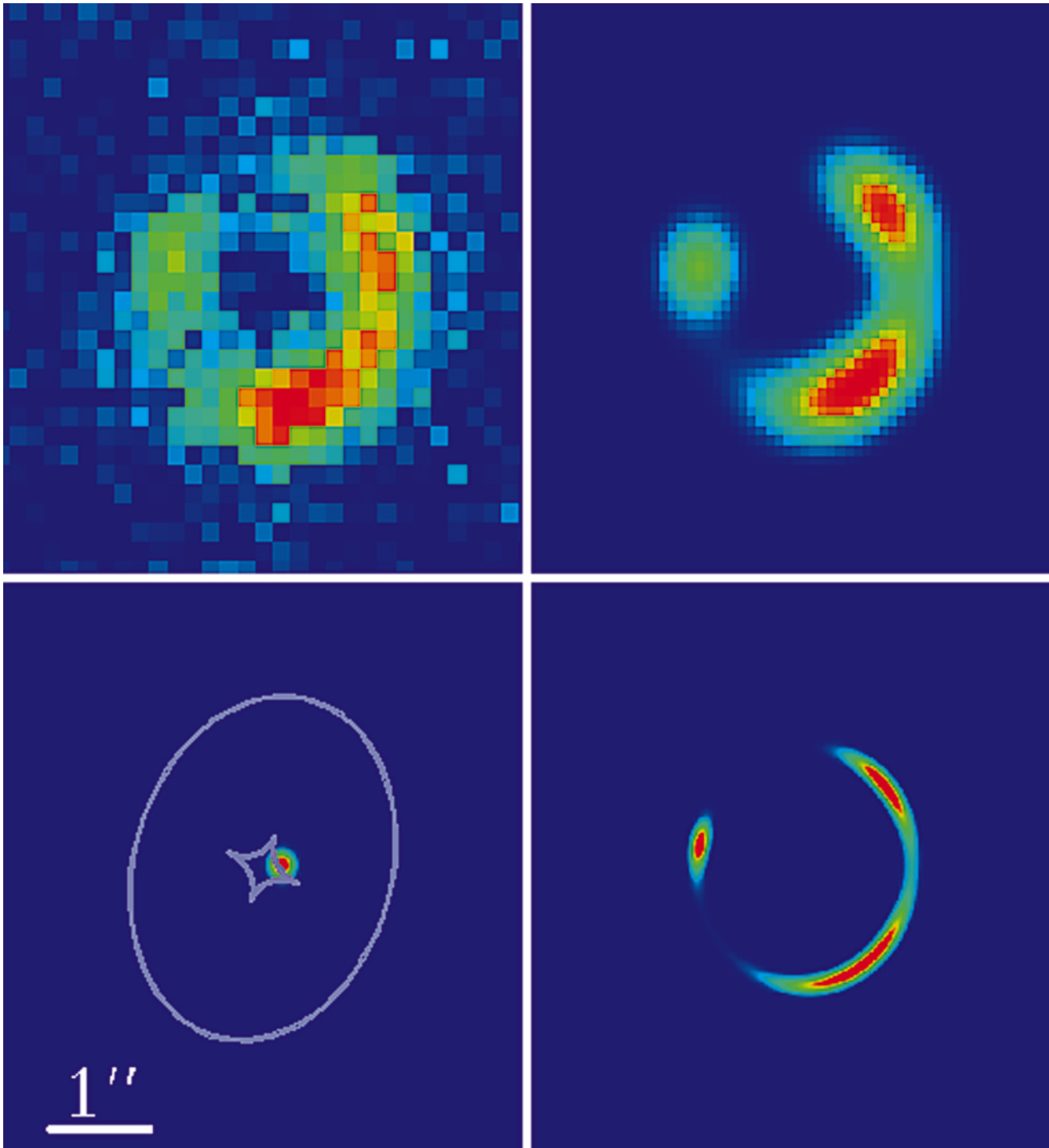


**Fig. 2.** False-colour images displaying the results of modelling the mass distribution in the lens. The size of each square image is  $5.5''$  on a side. North is up and East to the left. The top LH image shows the VLT Ly $\alpha$  image after subtraction of the image of the lensing galaxy, and rebinned to a pixel size of  $0''.18$ . The lower LH image shows the model of the source, and the 3-image and 5-image caustics. The lower RH image shows the image that would be observed at infinite spatial resolution, and the upper RH image is the lower RH image convolved with the psf to emulate the observing conditions. The upper RH image therefore models the upper LH image with zero noise. The good correspondence of the two upper images gives a measure of the accuracy of the mass model.

ber 12 and 13. The pixel size was  $0''.286$ . The final image is a mosaic from two positions, one centred on 0047–2808, total integration time 15 120 sec, and another at a position  $58''$  to the

SSW centred on a second distant elliptical, total integration time 4725 sec. At each position several sequences of 9-point dithers were summed. The seeing averaged  $0''.7$ . The data were flat–

fielded using a sequence of twilight sky exposures, and then an appropriate sky frame, formed from a running median filter through the stack of images, was subtracted from each data frame, and the resulting frames registered and summed.

### 2.3. Results

Fig. 1 shows the *rgb* colour image resulting from combining the *B* (*=b*), *Ly $\alpha$*  (*=g*), and *K* (*=r*) images. The ring stands out strongly in green because of the strong *Ly $\alpha$*  line in the narrow-band filter, while the lensing galaxy is very red and is visible inside the ring. A minimum  $\chi^2$  fit of a de Vaucouleurs model for the light profile of the lensing galaxy in the *K*-band image was computed by convolving two-dimensional  $r^{-1/4}$  profiles with the psf, measured from a star in the frame. (The *K*-band image is best for fitting the galaxy profile because the ring is not detected at this wavelength, and the contrast between the galaxy and the ring is maximised.) The model was then convolved with the *Ly $\alpha$* -band psf, scaled to the central counts in the *Ly $\alpha$*  image, and subtracted. The resulting image of the ring, rebinned to a pixel size of  $0''.18$ , is shown in the top left-hand panel of Fig. 2.

### 3. Gravitational lens model

Compared with the original NTT image (Warren et al. 1996a) the new VLT image has much higher signal-to-noise ratio. The counter image predicted by our original model, but not convincingly detected in the NTT image, is now clearly seen. The same modelling procedure as described in Warren et al. (1996a), where the projected surface mass density was assumed to follow the (intrinsic) de Vaucouleurs profile, now measured from the *K*-band image (as described above), has been applied. The single free parameter is the global mass-to-light ratio (M/L).

Utilising the computational technique for arbitrary lenses with elliptical symmetry (Schramm 1994) the M/L ratio in the model was adjusted to produce the most compact configuration for the unlensed image in the source plane. Here we briefly review the key steps in the procedure; a position in the image plane, represented by the complex coordinate  $z$ , is mapped onto the source plane position  $\omega$ , according to

$$\omega(z, \bar{z}) = z - \nabla \Phi(z, \bar{z}), \quad (1)$$

where  $\nabla = 2\partial/\partial\bar{z}$ . The deflection potential,  $\Phi$ , is related to the projected surface mass density in the lens,  $\Sigma$ , by

$$\nabla^2 \Phi(z, \bar{z}) = 2\Sigma(z, \bar{z})/\Sigma_{\text{crit}} \quad (2)$$

where  $\Sigma_{\text{crit}}$  is the critical surface mass density to gravitational lensing and is given by

$$\Sigma_{\text{crit}} = \frac{c^2}{4\pi G} \frac{D_{\text{os}}}{D_{\text{oI}}D_{\text{Is}}}. \quad (3)$$

Here,  $D_{ij}$  are the angular diameter distances between the source (s), lens (l) and observer (o) (Schneider et al. 1992).

A  $61 \times 61$  pixel ( $5.5 \times 5.5''$ ) region of the VLT narrow-band image, centred on the galaxy, was used for the computation. Assuming a fiducial value of M/L, the mapping given in Eq. 1

gives the coordinates in the source plane of any image-plane coordinate. The M/L was adjusted, focusing the emission over the source plane into a small region. This determines the centroid of the source. The source was then modelled as a Gaussian profile. The structure in the ring (i.e. the angular extent of the gaps, size of the counterimage) is dictated by the angular extent of the source. A source of FWHM of  $0''.2$  when reimaged by the lensing potential was found to reproduce the structure in the ring well. To reimage the source each pixel was sub-pixelated into a  $10 \times 10$  grid; these grid points were mapped to the source plane to measure the surface brightness at each grid point. Mapping of the surface brightness in this way is accurate provided the grid spacing mapped to the source plane is substantially smaller than the scale over which the surface brightness of the source varies.

Having fixed the source position and profile the lens M/L was then finely readjusted to provide the best fit, in terms of  $\chi^2$ , of the model of the ring to the data. The results of this procedure are presented in Fig. 2. The upper left-hand panel presents the VLT image of the ring after subtraction of the model for the surface brightness distribution of the foreground galaxy. Below, the model source is shown on the same scale together with the caustic lines defined by the gravitational lens model; the caustics delineate the regions of multiple imaging over the source plane. The resultant image for this source configuration is presented in the lower right-hand panel. In the upper right-hand panel this image has been convolved with a Gaussian seeing profile to approximate the observing conditions. There is good correspondence between the structure in the model and the observed structure of the ring.

The measured angular radius of the ring in the VLT image is  $1''.08 \pm 0.03$ . This more accurate value is smaller than the value measured from the NTT image ( $1''.35 \pm 0.1$ ) by 20% and this significantly lowers the mass estimate. Part of the discrepancy between the two measurements is due to the fact that the ring is elliptical in shape and that the counterimage (invisible in the old data) lies on the minor axis i.e. the old value for the radius was measured along the major axis of the ellipse. The two measurements are consistent therefore. The computed mass within the Einstein radius is  $1.73(1.95) \times 10^{11} h^{-1} M_{\odot}$  for  $q_o = 0.5(0.1)^1$ . The uncertainty in the mass estimate within the Einstein radius is dominated by the uncertainty in the radius rather than the form of the mass profile. Changing the radius by  $0''.06$  (i.e.  $2\sigma$ ) changes the computed mass by 10%. The M/L ratio for the model, corrected for luminosity evolution (Paper I), is  $M/L_{B(0)} = 14.2 h(12.1 h)$ .

*Acknowledgements.* We are grateful to the ESO UT1 Science Verification team for providing the optical data. GFL acknowledges support from the Pacific Institute for Mathematical Sciences (1998-1999). The authors acknowledge the data and analysis facilities provided by the Starlink Project which is run by CCLRC on behalf of PPARC.

<sup>1</sup>  $h$  is the Hubble constant in units of  $100 \text{ km s}^{-1} \text{ Mpc}^{-1}$

**References**

- Kochanek C. S., 1995, *ApJ*, 445, 559
- Leibundgut B., de Marchi G., Renzini A., 1998, *The Messenger*, 92, 5
- Miralda–Escudé J., Lehár J., 1992, *MNRAS*, 259, 31P
- Schneider P., Ehlers J., Falco, E. E., 1992, *Gravitational Lenses*, (Springer-Verlag, Berlin)
- Schramm, T., 1994, *A&A*, 284, 44
- Steidel C.C., Giavalisco M., Pettini M., Dickinson M., Adelberger K.L., 1996, *ApJ*, 462, L17
- Warren S. J., Hewett P. C., Lewis G. F., Møller P., Iovino A., Shaver P. A., 1996a, *MNRAS*, 278, 139
- Warren S.J., Hewett P.C., Lewis G.F., Møller P., Iovino A., Shaver P.A., 1996b, in C.S. Kochanek and J.N. Hewitt (eds), *Astrophysical Applications of Gravitational Lensing*, (Kluwer, Dordrecht), p. 329
- Warren S. J., Iovino, A., Hewett P. C., Shaver P. A., 1998, *MNRAS*, 299, 1215